Dislocations and the de Haas-van Alphen Effect in Copper*

D. W. Terwilliger† and R. J. Higgins
Department of Physics, University of Oregon, Eugene, Oregon 97403
(Received 31 May 1972)

Experiments have been carried out to determine the effect of lattice dislocations in pure copper single crystals on the de Haas–van Alphen (dHvA) scattering (Dingle) temperature X. The measurements were made on copper samples of measured dislocation density under stringent experimental conditions, including a magnetic field homogeneity of better than 2 ppm and an orientation of the sample symmetry direction along the field to within 0.05°. The results for the [111] neck and belly orbits in copper showed a linear dependence of X on the dislocation density D over the range $D \simeq 0.5\times10^{7}$ to 7×10^{7} cm^{-2}, with slopes given by $X_n/D \simeq 0.32\times10^{-7}$ K cm^2 and $X_b/D \simeq 0.08\times10^{-7}$ K cm^2. Two approaches have been suggested to explain the results: (i) The scattering temperature is inversely proportional to the electron relaxation time and is therefore a direct measure of electron scattering from dislocations; (ii) X is due to phase cancellation in the dHvA signal from orbits moving within the spatially varying elastic strain field of the dislocation array. The experimental results are discussed in terms of these two points of view.

I. INTRODUCTION

In a letter[1] (referred to later as TH), we reported preliminary results showing how a controlled array of lattice dislocations affects the amplitude of the de Haas–van Alphen (dHvA) effect, as measured by the Dingle scattering "temperature" X. We present those results more extensively here, including more data and a more reliable estimate of the uncertainty in the measured X and the dislocation density D, and of background effects in X. Dislocations which affect the residual resistance ratio (RRR) very little have a major effect on X, and the density of dislocations introduced in crystal growth or by handling may be sufficient to obscure the results, for example, of an impurity-scattering study. A collection of techniques developed in this experiment for the reliable measurement of the dHvA scattering temperature, including methods for characterizing dislocation density and crystalline substructure, has been published separately.[2,3]

After the TH letter appeared, Coleridge and Watts (CW)[4] published the results of a similar study. Watts[5] analyzed how such results may be related to phase-smearing effects[6] on a microscopic scale, due to the spatially varying dislocation strain field and to the sensitivity of the Fermi surface (FS) to strain. It was shown[4] that the Watts theory could be adjusted to fit the TH results well, fitting the CW results (with rather less data and some inhomogeneity of D) rather less well. The parameters coming from the fit were in plausible agreement with what would be estimated from the existing data on FS sensitivity to homogeneous elastic strain.[7]

Viewed simply as scattering, the TH results give a scattering rate in X of the order of 10^4 times that obtained from dislocation resistivity. This suggests that most dislocation scattering is by small angles, since X measures Landau level width or true lifetime, unweighted by scattering angle as in resistivity. The X values vary with orbit, largest at the neck and smallest on the belly, with $X_n/X_b \gtrsim 4$. In order to decide whether these results are useful input to the old and unsolved problem of electron scattering by lattice dislocations,[8] it is essential to test the Watts phase-smearing explanation. This explanation predicts that X will vary with magnetic field as $1/B$, owing to the assumption of a Gaussian strain distribution. It also predicts that X will vary with dislocation density as $D^{1/2}$, owing essentially to the variation of a scaling parameter (orbit size/dislocation spacing). Neither of these predictions has had a clear test. Since the TH data cover a large number (~ 30) of samples with stringent control of sample characterization, they should aid in assessing the current status of the problem.

II. EXPERIMENTAL

A variety of experimental techniques were developed for this study which are important in any application of the dHvA effect to the study of scattering. Since these techniques are described elsewhere,[2] this section will merely list relevant features. The magnetic field was produced by a 55-kG superconducting solenoid. The homogeneity was trimmed to 2 parts in 10^6 over the sample, eliminating that source of phase-smearing error. The samples were immersed in liquid helium, typically at 1.2 K, measured by He vapor pressure, and controlled to better than 0.02 K. The samples were oriented during the experiment so that the field was along the [111] direction within 0.05°, minimizing that source of phase-smearing

error. Measurements were made using the field-modulation technique[9] and second-harmonic detection, and the modulation field amplitude was controlled to vary as H^2. The modulation amplitude H_m was adjusted to peak the amplitude $J_2(2\pi \times FH_m/H^2)$ of the dHvA signal under study. Thus, the quantity recorded was very nearly the *first harmonic* of the dHvA amplitude, eliminating possible errors due to differing field dependence of harmonic amplitudes. In addition, data were recorded only at field values below which magnetic interaction effects were absent, as determined by a separate measurement of the d^2M/dH^2 waveform under small-modulation conditions. The modulation frequency (100 Hz) was chosen low enough that the modulation field completely penetrated the samples (determined by a separate experiment), eliminating possible errors in amplitude due to the field dependence of ths skin depth. The scattering temperature X was determined from the field dependence of amplitudes $A(H)$:

$$\ln[A(H)\sinh(KT/H)H^{1/2}] = \text{const} - KX/H \ , \qquad K = (2\pi^2 m_0 c\, k_B/e\hbar)\, m^*/m_0 \ . \tag{1}$$

Samples were acid cut (to minimize cutting damage and consequent amplitude errors in X) from commercial crystals[10] whose residual resistance ratio (after oxygen annealing[11]) was typically 2500, giving a residual impurity $X_i < 0.05$ K, as estimated from separate measurements on dirtier samples.[2] Substructure and dislocation density were characterized by surface etching and metallography,[12] with occasional checks that the surface was indicative of the bulk. Samples were selected from regions where the subgrain size was larger than the sample size, minimizing possible phase-smearing errors from this source. Dislocations were introduced by a double-bending technique, giving an array of edge dislocations whose Burgers vector $\vec{b}$ was $[\bar{1}01]$ and whose density was varied by varying the bend radius. The axis of the bar was cut 7° from $[0\bar{1}1]$, ensuring single slip. Bars with evidence of cross slip or dislocation clumping were rejected, since in that case the amplitude would be determined predominately by the more-dislocation-free regions. The bending technique, though advantageous in creating a well-defined dislocation array, is a potential source of phase-smearing error if the crystal orientation then varies within the sample. Double bending removes this problem on a macroscopic scale, since the bar ends up straight. Nature provides a check that this is true also on a microscopic scale since the belly-orbit amplitude is most sensitive to bending [$(d^2F/d\theta^2)$ is large], yet is relatively insensitive to dislocations. The neck orbit had X values at least four times larger, yet was insensitive to bending. Therefore, any failure to achieve a straight sample showed up as an irreproducible increase in X_b. A sufficient check on the delicacy of other aspects of sample handling is the observation that in samples with low D and high purity the measured X was essentially zero.

III. RESULTS

The principal results of the experiment are shown in Fig. 1, a plot of the dHvA scattering temperature X as a function of dislocation density D for [111] neck and belly orbits in copper. The numerical results are listed in Table I, which includes RRR and dislocation density for each sample, as well as the magnetic field range and the root-mean-square deviation (RMSD) of the amplitude data from a straight line used to calculate X.

Most samples listed in the table were taken from a crystal labeled 812, of initial dislocation density 4×10^5 cm^{-2} and RRR 2500. Samples 1 and 2 in Table I, however, represent X measurements made on very-low-D samples from a Czochralski crystal. These measurements, made early in the experiments, were used to demonstrate that copper crystals of sufficient purity (RRR > 4000) and perfection ($D < 10^5$ cm^{-2}) have essentially zero scattering temperatures; that is, $X = 0.05 \pm 0.05$ K. This substantiates the work of Phillips and Gold,[13] who found similar results in very pure and carefully prepared single crystals of lead, but did not directly characterize the actual state of perfection of the samples. In addition to setting a lower limit to D for the later experiments, these tests confirmed that the sample-preparation techniques were sufficiently gentle.

The data of CW,[4] also shown in Fig. 1, appear to fall below our results, especially for the neck orbit (where the results are most reliable). This may reflect a difference in the orientation of the dislocation array. In our samples, the bending geometry ensures single slip and an array of edge dislocations whose Burgers vector $\vec{b}$ lies along $[\bar{1}01]$. The dislocation lines would ideally lie along an *average* direction of [121], which is 19° from the magnetic field direction during the X measurement. The electron orbits are thus situated so as to suffer maximum disturbance from the plane strain field of the dislocation array.[8] In the CW experiment, by contrast, the dislocations were introduced by uniaxial compression or by spark erosion, and neither ensures single slip. The electron orbits would then sample a strain field whose plane may vary randomly. This would give a lower average scattering, as suggested both by classical ($H = 0$) dislocation scattering calculations[8] and by Pippard's phase-coherence arguments.[14] However, a quantitative estimate of this difference

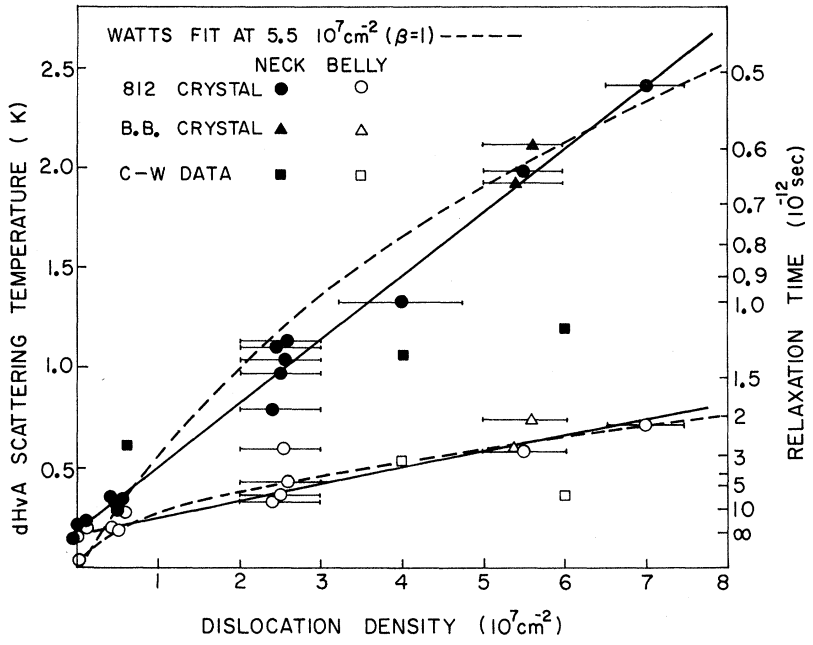

FIG. 1. Neck (closed circle, closed triangle) and belly (open circle, open triangle) dHvA scattering temperatures in copper as a function of sample dislocation density. The straight lines are least-squares fit to the X results. The scale on the right for the electron relaxation time, calculated from $X=\hbar/2\pi k\tau$, is displaced upward because of the background scattering for these samples discussed in the text. The curves are fits to the Watts theory (Ref. 5), selected in this example to pass through the data at $D=5.5\times10^7$ cm^{-2}. The uncertainty in the dislocation density of each sample is given in Table I; the uncertainty in X is less than 0.1 K. A preliminary version of this figure covering a narrower range of D and with less precision in the X values was published earlier (Ref. 1). Also shown (closed square, open square) are data from Ref. 4.

due to dislocation orientation would not be reliable at present, since any nonrandomness in the dislocation *density* (as noted by CW for their high-D sample) would also lower the average X measured.

In Fig. 1 the lines are a straight-line least-squares fit with slopes $X_n/D=0.32\times10^{-7}$ K cm^2 and $X_b/D=0.08\times10^{-7}$ K cm^2. Both lines intersect the X axis at about 0.18 K. A fit to the data leaving out the three lowest-D samples (30, 31, and 32) gave the same slopes and intercepts within 3% for the neck and 10% for the belly. The nonzero intercepts and the X measurements on low-D samples all suggest that a background X should be associated with the measurements on the samples from crystal 812. On the other hand, 0.18 K is somewhat higher than the impurity background in sam-

TABLE I. dHvA scattering-temperature results. The samples were prepared from crystal 812 except as noted.

Sample	RRR	D[a] (cm^{-2})	X_n (K)	Field range (kG)	RMSD (%)	X_b (K)	Field range (kG)	RMSD (%)
1[b]	4300	7×10^4	0.05	12–32	2.0	0.00	28–40	1.6
2[b]	4300	7×10^4	−0.01	12–26	0.5	0.02	24–38	1.0
30	2500	4×10^5	0.24	16–32	1.0	0.21	26–32	0.1
31	2500	4×10^5	0.15	15–25	2.4	0.16	24–32	2.1
32	2500	4×10^5	0.22	15–21	1.2	0.04	23–32	1.3
18	2500	5×10^6	0.36	18–38	0.6	0.20	25–41	1.7
19	2500	5×10^6	0.33	14–40	1.3	c	22–40	25.5
20	2500	5×10^6	0.29	15–37	1.4	0.19	23–35	1.4
21	2500	5×10^6	0.35	15–37	0.7	0.28	25–37	2.7
33	2500	$2–3\times10^7$	0.80	23–42	0.6	0.34	26–35	2.1
34	2500	$2–3\times10^7$	1.05	20–38	0.6	0.60	28–38	2.7
35	2500	$2–3\times10^7$	0.98	20–35	0.7	0.37	26–35	1.6
39	2500	$2–3\times10^7$	1.11	18–37	2.5	c	28–38	12.6
40	2500	$2–3\times10^7$	1.14	21–39	2.5	0.44	33–43	2.7
36	2500	4×10^7	1.34	24–37	0.7	c	30–37	7.0
37	2500	$5–6\times10^7$	1.99	28–43	1.3	0.59	35–46	2.2
38	2500	7×10^7	2.42	34–47	0.6	0.72	37–44	1.9
22[d]	5750	$5–6\times10^7$	1.93	33–41	0.2	0.60	35–43	3.1
23[d]	5750	$5–6\times10^7$	2.12	33–44	0.6	0.74	35–43	2.7

[a]Uncertainty in D is about ±10% unless otherwise indicated.

[b]From Czochralski crystal.

[c]Measurement of X_b was invalid since RMSD is greater than 4%, as discussed in Ref. 2.

[d]From blind-baffle crystal.

ples of RRR 2500, estimated to be less than 0.05 K. In providing a scale for the electron relaxation time on the right in Fig. 1, we have assumed that the measured background is real, and have set the bottom of the τ scale at 0.18 K. The τ scale is based on the assumption that the formula $X = \hbar/2\pi \times k\tau$ applies to the present case of X due to dislocations, a point which will be examined further in Sec. IV. The electron-relaxation-time anisotropy associated with [111] neck and belly electron orbits on the Fermi surface of copper can be estimated from the slopes of the lines in Fig. 1, giving

$$X_n/X_b = \tau_b/\tau_n \gtrsim 4 \ .$$

IV. DISCUSSION

The most striking result of the experiment is the large effect on the dHvA X produced by a dislocation array which would affect the resistivity very little. For example, for $D = 10^7$ cm^{-2},

$\tau_n \simeq 3.6\times10^{-12}$ sec (this work),

$\tau_b \simeq 1.5\times10^{-11}$ sec (this work),

$\tau_{\rm res} \simeq 4.0\times10^{-8}$ sec (Ref. 8).

This is indicative of the important role played by small-angle scattering events on the (phase-coherent) Landau level, whereas resistivity is sensitive only to large-angle (current-destroying) events.[8] The scattering angle required to destroy Landau level phase memory is approximately $1/n$, where n is the quantum number F/H. Although this result is well known,[15] no derivation appears to have been published, and it is instructive to consider the following geometrical example,[3] illustrated in Fig. 2. In a magnetic field an electron with quantum number n pursues an orbit of radius r where $2\pi r = n\lambda$ and λ is the de Broglie wavelength. Suppose that the electron begins an orbit at 0. If at point S the electron is deflected through a small angle θ into a new orbit a', then when the electron arrives back at 0, the total path will be longer than $n\lambda$ by

$$\delta = a' - a = (2\pi - \phi)r - \phi r = 2r\theta \ , \tag{2}$$

i.e.,

$$\theta = \delta/2r = \pi\delta/n\lambda \ . \tag{3}$$

If δ is larger than $\lambda/2$, the contribution of this orbit to the dHvA amplitude will be out of phase. Thus a scattering angle of $\theta = \pi\delta/n\lambda = \pi/2n \simeq 1/n$ may be catastrophic as measured by the dHvA τ. At 30 kG, for example, phase coherence will be destroyed by scattering through angles greater than 0.08° for neck orbits and 0.003° for belly orbits. A similar calculation for scattering out of the plane of the orbit gives a critical angle for elastic scattering into the adjacent Landau level which varies as

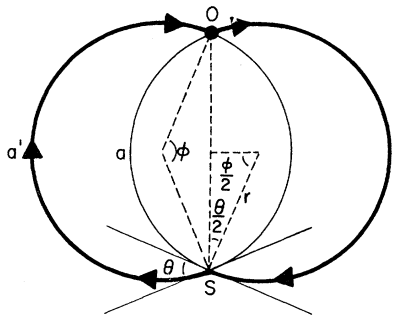

FIG. 2. Small-angle scattering and dephasing with a simple circular-orbit model.

$$\theta_{\parallel} \simeq \Delta p_{\parallel}/p_{\perp} \simeq (n\,\partial^2 A_F/\partial p_{\parallel}^2)^{-1/2} \ , \tag{4}$$

so that except for unusually narrow extrema, scattering in the plane will dominate, since $n \gg n^{1/2}$ ($n > 10^3$ for the orbits under consideration). Adopting this notion of a scattering event for the present, a rough estimate of the scattering cross section follows from a semiclassical argument.[3] In this experiment the dislocations formed a nearly parallel array, with the electron path nearly perpendicular to this "forest" of line defects. The geometry is that of a two-dimensional scattering problem, with the notion of a scattering "width" replacing "cross section." An expression for this width w follows from classical scattering theory:

$$w = (D v \tau)^{-1} \ , \tag{5}$$

where D is dislocation density, v is electron velocity, and τ is determined from the dHvA X measurement. Using published values of v,[16] one obtains scattering widths w of 4.5×10^4 and 5.6×10^3 Å for neck and belly orbits, respectively.[17] There is thus a factor-of-10 difference in the range of the dislocation strain field seen by electrons on these two portions of the Fermi surface. The direction of this anisotropy follows the pattern observed by Koch and Doezema[18] in surface-state scattering by *phonons*, and we note that it is possible to describe the dislocation strain field as a linear combination of phonons. The direction of the anisotropy also follows that observed for the response of FS *cross section* to a *homogeneous* elastic strain field.[7] These experimental results are similar in showing the neck electrons most tightly coupled to the lattice, and hence to disturbances in lattice periodicity.

The connection between the response of the FS to a homogeneous strain and the effect of lattice dislocations on the dHvA amplitude has been made by Watts[5] in a phase-smearing calculation using a simple model. There are two regimes, depending on the ratio of orbit size r to dislocation spacing d. For $r/d \ll 1$, the strain is essentially constant within an orbit, but each orbit samples a different

strain, which when averaged over the crystal gives a reduction in dHvA amplitude due to phase smearing. In this regime, what one operationally defines as X varies linearly with D, but because of the assumption of a Gaussian strain distribution, also shows a variation with magnetic field as $1/B$. For $r/d \gg 1$, however, the strain varies within individual orbits, and Watts computes the dephasing assuming a Gaussian form for the strain correlation function. In this regime, X varies as $D^{1/2}$ and displays little dependence on B. In fitting their data and also those of TH to this theory, CW[4] extract parameters measuring the sensitivity of various orbits to strain which are in plausible agreement with available data from homogeneously strained samples.[7] However, the values of these parameters (and hence the self-consistency of the theory) are sensitive to the form of the assumed strain distribution, and it is of interest to see to what extent the present data are consistent with the Watts assumptions. The complete form of the Watts expression [Ref. 5(b), Eq. (10)], which has the features mentioned above in appropriate regimes, has been fit to the $X(D)$ data, as shown by the curves on Fig. 1. The parameters which result are shown in Table II. The root-mean-square deviation of the data is somewhat greater for the Watts function than for a simple straight-line fit,

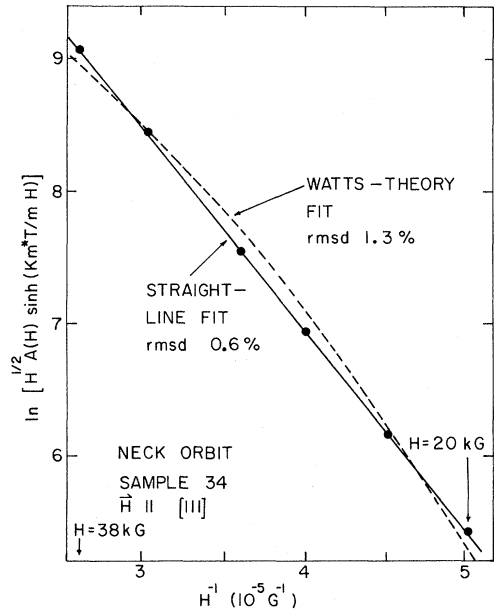

FIG. 3. Search for field dependence in the scattering temperature of the neck orbit. The example chosen covers the widest field range used in this experiment. The data points have been fitted both to a straight line (solid line) and to the Watts theory (dashed curve). The results are compared in Table II.

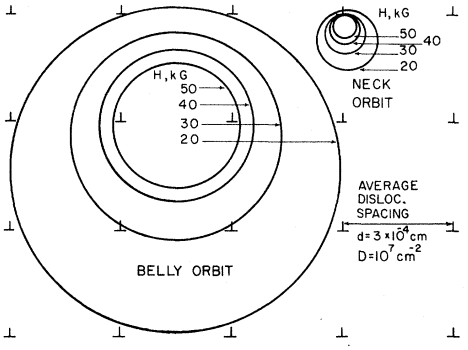

FIG. 4. Relative sizes of dislocation spacing and orbits. In this example, the dislocation density D is 10^7 cm^{-2} and the orbits are sketched for values of magnetic field appropriate to this experiment.

and there is no clear evidence for the turnover in X at high D. The CW data did show such a turnover at high D which was *greater* than the Watts theory, but was ascribed by CW to inhomogeneity in the dislocation array. This is confirmed by the present data, from samples selected for uniform D. The Watts expression has also been fitted to the amplitude as a function of $1/H$ to look for field dependence of X, as shown in Fig. 3. The Watts theory predicts a departure from linearity somewhat greater than that observed, but the discrepancy is only slightly larger (Table II) than the statistical uncertainty.[19] Thus, the validity of Watts's Gaussian strain distribution remains without a critical test.

We feel that the phase-smearing notions described by Watts and Coleridge describe the physical origin of the effect of lattice dislocations on the dHvA effect, and, rather than replacing scattering as an explanation for the observations, supply an intuitive approach to describe such small-angle scattering. Although the original scattering calculation of Dingle[20] has been more rigorously rederived,[21] even recent calculations appear appropriate only for memory-destroying (large-angle) and not diffusive (small-angle) collisions. The results of dHvA experiments may go beyond this present limitation of the theory to characterize experimentally the Landau level *line shape*. This is a more fundamental quantity, since the Dingle temperature X is meaningful only when the line shape is Lorentzian. Two such conclusions follow for the case of lattice-dislocation scattering.

(i) The distinction between phase smearing and small-angle scattering is not clear cut. In resonance experiments such as ESR, by contrast, the line shape is used to extract scattering information, and the distinction is made between homogeneous broadening (lifetime of states on atoms) and

inhomogeneous broadening (different resonance energy on different atoms due to inhomogeneous environment). Such a distinction is appropriate in the case of Landau levels only in the limit when the orbit size is small compared to both the defect range and spacing. This limit is not achieved in the present experiments, as shown in Fig. 4. Because the dislocation strain field is long range $(1/r)$, dephasing occurs *within* individual orbits. There appears to be no qualitative difference between this point of view and the notion of small-angle scattering. The principal uncertainty in the Watts dephasing calculation appears to be the assumption of a Gaussian distribution for the strain correlation function seen by an electron within an orbit. This corresponds to a random-phase approximation, yet the strain field sampled by electrons in neck orbits appears far from random, following a well-defined $(1/r)$ form.

(ii) The magnitude of X due to a given line-broadening event depends not only on the linewidth,

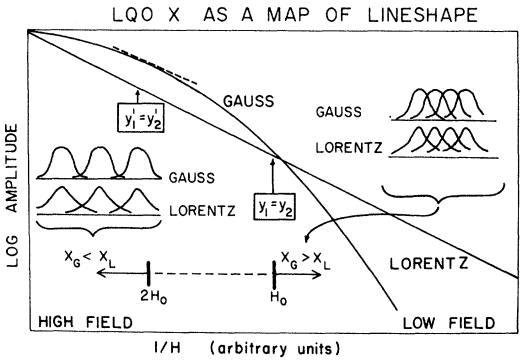

FIG. 5. Field dependence of the Landau-quantum-oscillation amplitude for two examples of Landau level line shape, the usual Lorentzian (simple scattering) and the Gaussian (random distribution of dephasing). The curves cross when the linewidth equals the Landau level spacing. The scattering temperature X, measured as the slope, is equal in the two cases only at one point, shown as the dashed line. A non-Lorentzian line shape should show up as a departure from linearity, which in practice may be obscured by the finite range of H covered in most experiments.

but also upon the form of the broadening function. An example is shown in Fig. 5, comparing Lorentzian and Gaussian line broadening. The curves cross when the Landau level spacing equals the linewidth, a result which is independent of line shape. This follows because the quantity measured in a Landau quantum oscillation (LQO) experiment is essentially the Fourier transform of the Landau level spectrum. If the line shape is Gaussian, what one measures as X (the *slope* of Fig. 5) depends on the magnetic field, and equals the Lorentzian X only at $H = 2H_0$, where H_0 is the crossing field in Fig. 5. Thus, in extracting from X parameters characterizing the coupling of orbit to scattering center, the results are sensitive to the correct choice of line shape. The examples selected in Fig. 5 are the appropriate limiting cases for the dislocation-scattering problem, but the existing data (e.g., Fig. 3) do not cover a wide enough field range to distinguish between them. Such an experiment is now in progress.[22] Alternatively, a measure of the Landau level line shape may be extracted from the relative amplitudes of the dHvA harmonics. This approach is of special value in cases such as the magnetic-impurity problem, where energy dependence of the relaxation time has as a consequence a strong field dependence in X and a strong departure from Lorentzian line shape. Such an experiment is now in progress, using on-line computer waveform analysis to extract X.[23]

TABLE II. Orbit parameters and summary of scattering-temperature results.

Parameter	Orbit: Neck	Orbit: Belly
de Broglie wavelength (Å)	55	10.5
"Racetrack" width (Å)	300	300
Orbit diameter ($H = 3\times10^4$ G) (Å)	12×10^3	60×10^3
Average dislocation spacing ($D = 10^7$ cm^{-2}) (Å)	30×10^3	30×10^3
$[X/D]$ (10^{-7} K cm^2), linear fit	0.32	0.08
Scattering "width" from X (Å)	45×10^3	5.6×10^3
X vs D, RMSD (K)		
linear fit to Fig. 1	0.04	0.01
Watts-theory fit to Fig. 1	0.06-0.09	0.02
Dephasing parameter μ[a]		
Watts-theory fit to Fig. 1	11–16	0.8–1.2
Ref. 4 results	15–19	0.9–1.3
X vs $1/H$, RMSD (percent)[b]		
linear fit to Fig. 3	0.6	...
Watts-theory fit to Fig. 3	1.3	...

[a] $\mu = 1$ for a free-electron gas. The range of parameters shown covers a range of assumptions in the Watts theory (correlation length/dislocation spacing; array correlated/uncorrelated). The present values are lower than those in Ref. 4 principally because of the nonzero impurity background X_1, which was included in the fit.

[b] Here the RMSD is evaluated for the linear fit to the function defined in Eq. (1). The values quoted in percent here and in Table I are calculated from the root-mean-square deviation equal to

$$100\left(\sum_{i=1}\frac{(y_i - KX/H_i)^2}{N}\right)^{1/2},$$

where y_i is the left-hand side of Eq. (1). This form is chosen since the *absolute* error in the ln term of Eq. (1) is dominated by the *fractional* uncertainty in measuring A, as discussed in Ref. 2. For purposes of comparison, the same definition of RMSD was used for the Watts fit shown in Fig. 3.

ACKNOWLEDGMENTS

We wish to thank Y. K. Chang for his help in many phases of sample preparation and data analy-

sis and Hal Alles for assistance in the construction of the small-angle rotator. We also acknowledge helpful discussions from numerous colleagues, including J. McClure, G. Wannier, P. Coleridge, B. Watts, M. Wortis, and D. H. Lowndes.

---

*Research supported by the National Science Foundation under Grant No. GP-25532.

†Present address: Department of Physics, Middlebury College, Middlebury, Vt. 05753.

[1]D. W. Terwilliger and R. J. Higgins, Phys. Letters 31A, 316 (1970); R. J. Higgins, D. W. Terwilliger, and Y. K. Chang, in *Proceedings of the Twelfth International Conference on Low Temperature Physics*, edited by E. Kanda (Keigaku, Tokyo, 1971), p. 605.

[2]D. W. Terwilliger and R. J. Higgins, J. Appl. Phys. 43, 3346 (1972).

[3]D. W. Terwilliger, thesis (University of Oregon, 1970) (unpublished; available from University Microfilms, Ann Arbor, Michigan, dissertation No. 71-1354).

[4]P. T. Coleridge and B. R. Watts, in *Proceedings of the Twelfth International Conference on Low Temperature Physics*, Ref. 1, p. 611; Phil. Mag. 24, 1163 (1971).

[5](a) B. R. Watts, in *Proceedings of the Twelfth International Conference on Low Temperature Physics*, Ref. 1, p. 609; (b) Phil. Mag. 24, 1151 (1971).

[6]D. Shoenberg, Physik Kondensierten Materie 9, 1 (1969); see also M. Springford, Advan. Phys. 20, 493 (1971).

[7]D. Shoenberg and B. R. Watts, Phil. Mag. 15, 1275 (1967).

[8]Z. S. Basinski, J. S. Dugdale, and A. Howie, Phil. Mag. 8, 1989 (1963); R. A. Brown, Phys. Rev. 156, 692 (1967); *The Physics of Metals, Vol. 1, Electrons*, edited by J. M. Ziman (Cambridge U. P., New York, 1969), p. 264.

[9]D. Shoenberg and P. J. Stiles, Proc. Roy. Soc. (London) A281, 62 (1964); A. Goldstein, S. J. Williamson, and S. Foner, Rev. Sci. Instr. 36, 1356 (1965); R. W. Stark and L. R. Windmiller, Cryogenics 8, 272 (1968); L. R. Windmiller and J. B. Ketterson, Rev. Sci. Instr. 39, 1672 (1968).

[10]Research Crystals Inc., Richmond, Va.

[11]J. J. Gniewek and A. F. Clark, J. Appl. Phys. 36, 3358 (1965).

[12]J. D. Livingston, in *Direct Observation of Imperfections in Crystals*, edited by J. B. Newkirk and J. H. Wernick (Interscience, New York, 1962), pp. 115–130.

[13]R. A. Phillips and A. V. Gold, Phys. Rev. 178, 932 (1969).

[14]A. B. Pippard, Proc. Roy. Soc. (London) A287, 165 (1965).

[15]Cited, for example, by Shoenberg, Ref. 6.

[16]M. R. Halse, Phil. Trans. Roy. Soc. London 265, 507 (1969).

[17]Since these values are of the same order as the orbit diameter (Table II), yet the simple model assumes straight-line paths, the values are not expected to be quantitatively valid.

[18]J. F. Koch and R. E. Doezema, Phys. Rev. Letters 24, 507 (1970).

[19]Out of some 40 samples, larger deviations from linearity than that shown in Fig. 3 showed up only in a few cases for the belly orbit (Table I, Ref. c). Since the belly orbit has a smaller X, the curvature predicted by the Watts theory is smaller than that expected from the neck. The observed deviations from linearity in these cases were random rather than of uniform curvature, and nonreproducible from sample to sample, from which it was concluded they are due to crystalline substructure. Further discussion and an example are given in Ref. 2.

[20]R. B. Dingle, Proc. Roy. Soc. (London) A211, 517 (1952).

[21]A. D. Brailsford, Phys. Rev. 149, 456 (1966); Erich Mann, Physik Kondensierten Materie 12, 210 (1971); S. Engelsberg and G. Simpson, Phys. Rev. B 2, 1657 (1970).

[22]Y. K. Chang and R. J. Higgins, Bull. Am. Phys. Soc. 17, 40 (1972).

[23]Hal Alles and R. J. Higgins, Bull. Am. Phys. Soc. 17, 93 (1972).